

# On the Energy-Efficient of Throughput-Based Scheme Using Renewable Energy for Wireless Mesh Networks in Disaster Area

MENG LI<sup>1</sup>, (Student Member, IEEE), HIROKI NISHIYAMA<sup>1</sup>, (Senior Member, IEEE),  
NEI KATO<sup>1</sup>, (Fellow, IEEE), YASUNORI OWADA<sup>2</sup>, (Member, IEEE),  
AND KIYOSHI HAMAGUCHI<sup>2</sup>, (Member, IEEE)

<sup>1</sup>Graduate School of Information Sciences, Tohoku University, Sendai 980-8577, Japan

<sup>2</sup>National Institute of Information and Communication Technology, Sendai 980-0812, Japan

CORRESPONDING AUTHOR: M. LI (mengli@it.ecei.tohoku.ac.jp)

**ABSTRACT** We study the emergency communication problem in the post-disaster scenario. The emergence of Renewable Energy-enabled Based Station (REBS), which has pre-equipped energy harvesting devices, provides a new perspective to solve this problem, since the post-disaster communication scenario happens to be a Wireless Mesh Network (WMN) constituted by REBSs. However, one needs to address the unstable and inadequate power supply, insufficient capacities of the communication links, and the time-varying traffic demands accordingly during a period of time. In this paper, we deal with these problems and focus on optimizing data traffic throughput with the lowest weighted energy consumption based on the expectation of traffic demands. We firstly analyze the post-disaster communication issue and formulate this problem into a Mixed Integer Linear Programming (MILP) problem, and propose an off-line energy efficient scheme using the expectation of traffic demands. Furthermore, an on-line scheme is put forward which dynamically adjusts the off-line result with the knowledge of the current real data traffic demands. The efficiency of our proposal is demonstrated by theoretical analyses and numerical results.

**INDEX TERMS** Wireless mesh networks (WMNs), renewable energy-enabled base station (REBS), resource allocation, traffic distribution, time-slotted system.

## I. INTRODUCTION

The provision of network service in disaster area is considered crucial, since it is expected to help the relief effort by passing the information (i.e., position of sanctuaries) to the rescuers, as well as ensuring the communication demands of the people inside the disaster area. However, a principal challenge in post-disaster case is that due to the damage to the crucial infrastructures (i.e. power supply, network facilities), most of the original energy sources and network connection routes are no longer usable [1]–[3]. To add insult to the injuries, such condition is likely to last for some time [3]. Wireless Mesh Networks (WMNs) constituted by Renewable Energy-enabled Base Station (REBS) is regarded as an efficient alternative for the post-disaster scenario. In such network, harvesting facilities (i.e., solar panel, wind turbine) are used to yield energy from ambient environment. Before disaster, the REBSs use both of the non-renewable energy and renewable energy: the non-renewable energy from power

plant is firstly transmitted to the Microgrids and then distributed to the connecting REBS; the renewable energy is the one generated by energy harvesting facilities, all REBSs and Microgrids have such facilities, therefore the renewable energy for each REBS can be the local one (from its facility) or the remote one (from the Microgrids' facilities) [4]. When the non-renewable energy supply is cut due to the destruction, the REBSs in the network run entirely on renewable energy sources. Note that some connections between Microgrids and REBSs are also broken therefore only the local renewable energy is available for such REBSs. Movable and Deployable Resource Unit (MDRU) [3] is one of the existing solutions using vehicle-borne cellular which can provide emergency Internet connection and rapidly accommodate network services. These vehicle-based network gateways are usually deployed in the easy-rescue places such as the border of the disaster area, or directly connected to certain REBSs. The other REBSs use their interconnect facilities

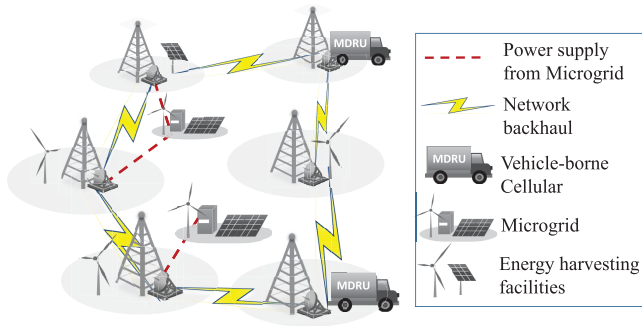


**FIGURE 1. System structure of the Wireless Mesh Network made up of Renewable Energy-enabled Base Station in post-disaster area.**

(i.e., microwave plate, long distance WiFi) [5], so as to interconnect each other and finally reach network gateways in a multiple-hop and multi-path manner. The considered system structure is shown in Fig. 1.

Although the above facilities for emergency usage meet the prerequisites for providing the basic network connection in disaster area, it still has a long way to design the scheme for providing the network services. There are several challenges that need to be addressed accordingly. The first one is the **limited and diverse energy supply**. In post-disaster area, each REBS has unique energy harvesting ability, and such ability is embodied in spatial and temporal, this is due to the different deployment places and weather conditions as time elapsed [6]. The second problem is the **mesh-feature of the transmission path**. Because of the damages, each REBS has to rely on neighbors to relay its data to the gateways, instead of the direct transmission. In post-disaster case, the destruction of transmission links forces us to explore the possible multiple paths from each REBS to the gateways. The third problem is the **provision of long-term energy-efficient throughput-maximization**. According to [3], network will experience a sharp increase of data traffic demands after disaster. The provision of high system throughput guarantees the services such as VoIP, SMS and so forth, and should be considered in optimization. On the other hand, since the renewable energy is the only energy source for each REBS, keeping energy consumption as low as possible is also critical. We use weighted-energy consumption metric, which takes the energy harvesting abilities into consideration. Moreover, the optimization approach should cover a long-time span problem, since the rebuilt effort cannot be accomplished at once.

Recently, the disaster and REBS-related techniques have been extensively explored. Some previous work has been conducted for energy efficiency-related fields for cellular systems [7]–[9]. [10]–[13] later extended the work by using hybrid energy in REBS. Moreover, [14]–[18] considered the combination of energy and traffic distribution issue. However, the work [14]–[16] considered the ample network capacities or energy input, which would be luxuries in disaster, [17], [18] considered the limited resources but they

only focused on the optimization problem in a single time slot, which might lead to the unsatisfied result in the long run. Although such efforts are helpful in designing the network in causal case, the above research fails to consider the shortages of resources and long-term optimization in post-disaster case. In our previous work [19], we proposed a scheme that considers the joint optimization problem of data traffic distribution, energy allocation, and operating scheduling problem. However, the inaccuracy of data traffic demands is not taken into consideration.

To address the problem of a long-term energy-efficient throughput-maximization, with considering the characteristics of energy and network in disaster area, we firstly make use of the traffic expectation and propose an off-line scheme. Based on the real traffic demands, we bring forward an on-line scheme that dynamically adjusts the result of off-line scheme. The key contributions of this paper are summarized as follows:

- We focus on the joint optimization problem in REBS-based WMNs with limited battery capacity. We develop an optimization model that considers limited input energy and link capacity in a period of time. The problem model is demonstrated as a Mixed Integer Linear Programming (MILP) problem.
- Because energy is scarce in disaster area, we also consider energy efficiency in the proposed scheme. We introduce a metric, namely weighted energy-efficiency, to measure how much energy is consumed with consideration of energy harvesting ability. The optimization objective is to achieve the optimal system utility with a less weighted energy consumption than the other strategies that have the maximal system utility.
- We propose a two-stage off-line scheme using the expectation of traffic demands. Due to the possible imprecise estimation (overestimate or underestimate of data traffic demands), we further propose an on-line dynamic adjusting scheme that revises the result of off-line scheme in each time slot.
- We demonstrate the efficiency of the proposed scheme through theoretical and simulation studies, which prove that the proposed on-line scheme can achieve high efficiency even without precise traffic demands information.

The remainder of this paper is organized as follows. In section 2, we develop a model for the joint optimization of energy allocation and data traffic distribution of each REBS. In section 3, we propose the off-line solution and then make an on-line extension for the considered problem. The numerical results are demonstrated in section 4. Finally we conclude this paper in section 5.

## II. SYSTEM ASSUMPTIONS AND PROBLEM FORMULATION

In this section, we describe the related assumptions for the considered REBS-based WMN, define the network model in detail and introduce the optimization objective.

## A. SYSTEM ASSUMPTIONS

### 1) FOR THE INPUT ENERGY

As mentioned in previous section, the input energy generally falls into two categories, one is local input energy from its own energy harvesting facilities, the other is the energy from Microgrid. The differences among the positions of REBSs and the changing weather conditions cause spatial and temporal diversity of the energy harvesting abilities respectively. Because the input energy for each REBS is mostly determined by weather condition (i.e., illumination intensity), the input energy can be estimated beforehand by combining the knowledge of past experience and weather forecast. The related work of energy provision and prediction can be found in [6], [20], and [21]. We assume energy harvesting profiles of Microgrids and REBSs are known. Such technique may require the collaborative control with Wireless Sensor and Actuator Networks (WSANs) [22].

### 2) FOR DATA TRAFFIC DEMANDS

In post-disaster area, people tend to stay in temporary shelters (i.e., gymnasium) covered by REBSs. The data traffic demand there seems to be monotonous since users in this area may not frequently move. We assume we can estimate the traffic demand expectation, by combining the population covered by the REBS, the ratio of active users as the time collapse, the obtained previous traffic profile and so on [9]. It is noted such traffic demand expectation is not precise and will affect the result.

### 3) FOR THE NETWORK AND SYSTEM STRUCTURE

The state-of-edge vehicle-borne cellular gateway can provide almost infinite network capabilities to the outside [3]. The REBSs in the network are equipped with the interconnection facilities such as Microwave panel (i.e., MDR-8000) or long-distance WiFi (i.e., NanoBridge M2) [5], they have different deployment costs and can provide different connection capabilities. For each REBS, part of the input energy will be used for constant operating and activating subcarriers, and the rest will be stored in battery. The constant operating consumption is made up by the cooling, AC/DC converting and so on. The active subcarrier is the other factor that contributes the consumption, which is determined by the number of the active subcarriers. As compared to the above two factors, the energy used by the links between REBSs is not significant (i.e., the energy used by the links is less than 50W, while the constant operating consumption is 712.2W from [5] and [9]). Hence such kind of consumption can be neglected or included in the operating consumption as a small constant. The number of subcarriers also specifies the upper bound for uplink traffic of each REBS. Besides the local traffic demands, each REBS needs to relay the traffic sent by its neighbors. We define the system throughput as the amount of traffic pass through the gateways.

## B. OPTIMIZATION OBJECTIVE

Generally, system throughput is our major concern. Compared with energy requirement, the renewable energy

input is not adequate, therefore we also consider energy efficiency when fulfilling the maximal data traffic demands. Since the recharging rates among harvesting facilities are different, we use weighted energy consumption which takes energy harvesting ability into consideration, and is unlike the spectral efficiency in [23].

## C. TIME-SLOTTED SYSTEM

We use time-slotted system. Let  $[0, T_0)$  be the considered interval and  $T_0$  be the expected time when network can be reinstated. The interval is divided into discrete time samples  $\{t_1, t_2, \dots, t_T\}$ , and  $\mathcal{T} = \{t_1, t_2, \dots, t_T\}$  where  $T$ ,  $t_0$  and  $t_i$  is the number, the length and the index of time slot respectively. We assume traffic demand and energy harvesting ability of each REBS are stable in  $t_i$ .

## D. NETWORK MODEL

We use an undirected graph  $G(\mathcal{N}, \mathcal{C})$  to denote the network topology. Assume that there are  $N$  affected REBSs in the disaster area, and let  $\mathcal{N}$  ( $\mathcal{N} = \{n_1, n_2, \dots, n_N\}$ ) be the set of these REBSs, where  $|\mathcal{N}|=N$ . Let  $\mathcal{C}$  denote the set of interconnection links between REBSs, and  $c_{n_j}^{n_k}$  be the original capacity of link  $(n_j, n_k)$ . In this work, we assume the symmetrical links (i.e.,  $c_{n_j}^{n_k} = c_{n_k}^{n_j}$ ), and it can be easily extended to the asymmetrical case. Normally,  $c_{n_j}^{n_k}$  is constant therefore  $G(\mathcal{N}, \mathcal{C})$  is enough to represent the topology. However, due to limited energy input, REBSs may not be always active after disaster, hence the link capacities are also determined by the operating status of the associated REBSs. Let  $c_{(n_j, n_k)}(t_i)$  be the link capacity of  $(n_j, n_k)$  in  $t_i$ , and  $\rho_{n_j}(t_i)$  be the operating status of  $n_j$  in  $t_i$ , then  $c_{(n_j, n_k)}(t_i)$  is denoted as follows:

$$0 \leq c_{(n_j, n_k)}(t_i) \leq c_{n_j}^{n_k} \cdot \rho_{n_j}(t_i), \quad (1)$$

$$0 \leq c_{(n_j, n_k)}(t_i) \leq c_{n_j}^{n_k} \cdot \rho_{n_k}(t_i), \quad (2)$$

where  $\rho_{n_j}(t_i)$  is a boolean variable and it satisfies:

$$\rho_{n_j}(t_i) = \begin{cases} 1 & \text{if } n_j \text{ is active in } t_i, \\ 0 & \text{otherwise.} \end{cases} \quad (3)$$

When  $n_j$  is inactive in  $t_i$  ( $\rho_{n_j}(t_i) = 0$ ), it will stop operating. Eq. 1 and 2 demonstrate that the link is available iff the REBSs at the both ends are active.

Let  $\mathcal{G} = \{g_1, g_2, \dots, g_F\}$  be the set of gateways, where  $|\mathcal{G}| = F$  and  $\mathcal{G} \subset \mathcal{N}$ . Denote  $\mathcal{M}$  ( $\mathcal{M} = \{m_1, m_2, \dots, m_M\}$ ) as the set of Microgrids, and  $|\mathcal{M}| = M$ . Each  $m_k$  is connected to several REBSs, we denote the set of associated REBSs of  $m_k$  by  $M^{(m_k)} = \{n_1^{m_k}, n_2^{m_k}, \dots, n_i^{m_k} \in \mathcal{N}\}$ .

## E. ENERGY-RELATED MODEL

### 1) INPUT ENERGY

There are two kinds of input energy for each REBS. The local input energy can only be used locally, denote  $l_{n_j}(t_i)$  as such input of REBS  $n_j$  in  $t_i$ . The remote energy input is determined by connected Microgrids. Suppose the energy that Microgrid  $m_k$  can harvest during  $t_i$  is  $h^{m_k}(t_i)$ , and the amount of energy allocated to REBS  $n_j$  is  $h_{n_j}^{m_k}(t_i)$ . The received energy will be 0

if  $n_j$  is not connected to  $m_k$ . We have the following equation for  $m_k$ :

$$0 \leq \sum_{n_j \in \mathcal{M}^{(m_k)}} h_{n_j}^{m_k}(t_i) \leq h^{m_k}(t_i) + B_{m_k}(t_i), \quad (4)$$

where  $B_{m_k}(t_i)$  is residual energy of  $m_k$  at the beginning of  $t_i$ , and we will explain it in section 2.5.3. For REBS  $n_j$ , the energy input during  $t_i$  is the summation of the local energy and allocated remote energy:

$$H_{n_j}(t_i) = l_{n_j}(t_i) + \sum_{m_k \in \mathcal{M}} h_{n_j}^{m_k}(t_i). \quad (5)$$

For some REBSs, because of the devastation caused by disaster, their original connections to Microgrids are broken, and only local input energy is available for them.

## 2) ENERGY CONSUMPTION

The REBSs in post-disaster area rely on renewable energy to guarantee their operations. Let  $P_{n_j}(t_i)$  be the total energy consumed by REBS  $n_j$  in  $t_i$ . Subcarrier energy consumption is determined by the number of active subcarriers [9]: let  $s_{n_j}(t_i)$  ( $s_{n_j}(t_i) \in \mathbb{Z}^+$ ),  $e_s$  and  $e_0$  be the number of active subcarriers in  $t_i$ , energy requirement of each subcarrier, and constant operating energy consumption respectively. We neglect the constant transmission power between REBSs since it does not essentially affect our consideration.  $P_{n_j}(t_i)$  can be calculated as follows:

$$P_{n_j}(t_i) = [(s_{n_j}(t_i) \cdot e_s) + e_0] \cdot \rho_{n_j}(t_i), \quad (6)$$

$P_{n_j}(t_i)$  is firstly determined by  $\rho_{n_j}(t_i)$ : if  $n_j$  is inactive, there is no energy consumption in  $t_i$ , otherwise  $e_0$  is needed. If  $n_j$  is active, there can be another kind of energy consumption, which is determined by the number of activated subcarrier  $s_{n_j}(t_i)$ .  $s_{n_j}(t_i)$  should be less than the maximal number of subcarriers  $S$ .

## 3) ENERGY STORAGE

In order to store the residual harvested energy, each REBS is equipped with a battery that has finite capacity. Let  $B_{n_j}(t_i)$  denote the residual energy of  $n_j$ 's battery at the beginning of  $t_i$ .  $B_{n_j}(t_{i+1})$  equals  $B_{n_j}(t_i)$  plus the energy input in  $t_i$  and minus the consumed energy in  $t_i$ :

$$B_{n_j}(t_{i+1}) = B_{n_j}(t_i) + H_{n_j}(t_i) - P_{n_j}(t_i). \quad (7)$$

The battery capacity of REBS  $n_j$  is  $B_{n_j}^0$ , then  $B_{n_j}(t_i)$  should satisfy the following constraint:

$$0 \leq B_{n_j}(t_i) \leq B_{n_j}^0. \quad (8)$$

The battery capacity of Microgrid  $m_k$  is  $B_{m_k}^0$ , let  $B_{m_k}(t_i)$  denote the residual energy of  $m_k$ 's battery at the beginning of  $t_i$ . It should satisfy the following constraints:

$$0 \leq B_{m_k}(t_i) \leq B_{m_k}^0, \quad (9)$$

$$B_{m_k}(t_{i+1}) = B_{m_k}(t_i) + h^{m_k}(t_i) - \sum_{n_j \in \mathcal{M}^{(m_k)}} h_{n_j}^{m_k}(t_i). \quad (10)$$

## F. TRAFFIC MODEL

Suppose the expected uplink data traffic demand under the coverage of  $n_j$  in  $t_i$  is  $\bar{d}_{n_j}(t_i)$ , and let  $\epsilon_{n_j}(t_i)$  denote the gap between the real uplink data traffic demand of  $n_j$  in  $t_i$  and the estimated expectation. Hence the real data traffic demand,  $d_{n_j}(t_i)$ , can be denoted as follows:

$$d_{n_j}(t_i) = \bar{d}_{n_j}(t_i) + \epsilon_{n_j}(t_i). \quad (11)$$

Since  $d_{n_j}(t_i)$  cannot be precisely estimated, we suppose it is unknown to us in the very beginning (i.e., at time 0). At the beginning of time slot  $t_i$ , we know the exact demands in this time slot (i.e.,  $d_{n_j}(t_i)$  for all  $n_j \in \mathcal{N}$ ), which is widely accepted assumption [15], [17]. Since the long-term optimization needs to be addressed in the very beginning and we only know the expectation of traffic demands, we have to explore such value to obtain an acceptable result in the long run. We do not assume further traffic information (i.e., stochastic feature as in [24]) is available. In the remainder, unless clearly defined, the data traffic is the expected one.

Due to the limitation of energy and network capacity, REBSs in the considered network cannot keep enough subcarrier active all the time. As a result, REBSs may meet only part of uplink data traffic demands in certain time slots. Suppose the actual uplink data traffic of  $n_j$  in  $t_i$  is  $f_{n_j}(t_i)$ , it should satisfy the following constraints:

$$f_{n_j}(t_i) \leq \rho_{n_j}(t_i) \cdot s_{n_j}(t_i) \cdot r_0, \quad (12)$$

$$0 \leq f_{n_j}(t_i) \leq d_{n_j}(t_i), \quad (13)$$

where  $r_0$  denotes the achievable transmission rate when a subcarrier is active. Eq. 12 means the actual uplink traffic should not beyond uplink traffic capacity, which is proportional to the number of active subcarriers. Note that when we only have the traffic expectation,  $d_{n_j}(t_i)$  in Eq. 13 is replace by  $\bar{d}_{n_j}(t_i)$  in the computation.

Each REBS is also responsible for relaying the data traffic of other REBSs. Assume that  $f_{n_l}^{(n_j, n_k)}(t_i)$  is the actual uplink data traffic of REBS  $n_l$ , and is sent via link  $(n_j, n_k)$  in  $t_i$ . Therefore, the total traffic via link  $(n_j, n_k)$ , should be less than the link capacity:

$$f^{(n_j, n_k)}(t_i) = \sum_{n_l \in \mathcal{N}} f_{n_l}^{(n_j, n_k)}(t_i) \leq c_{(n_j, n_k)}(t_i). \quad (14)$$

For the non-gateway REBS  $n_j$ , it should send the local data traffic as well as the relayed traffic to the neighbor REBS or the connected gateways. If we consider this problem from the point of view of flow conservation, then the following equations should be satisfied:

$$\sum_{v \in \mathcal{N}} f_{n_j}^{(u, v)}(t_i) = 0, \forall u \in \mathcal{N} \setminus (\{n_j\} \cup \mathcal{G}), n_j \in \mathcal{N}, \quad (15)$$

$$f_{n_j}^{(u, v)}(t_i) = -f_{n_j}^{(v, u)}(t_i), \forall u, v, n_j \in \mathcal{N}, \quad (16)$$

$$f_{n_j}(t_i) = \sum_{u \in \mathcal{N} \setminus \{n_j\}} f_{n_j}^{(n_j, u)}(t_i), \forall n_j \in \mathcal{N}, \quad (17)$$

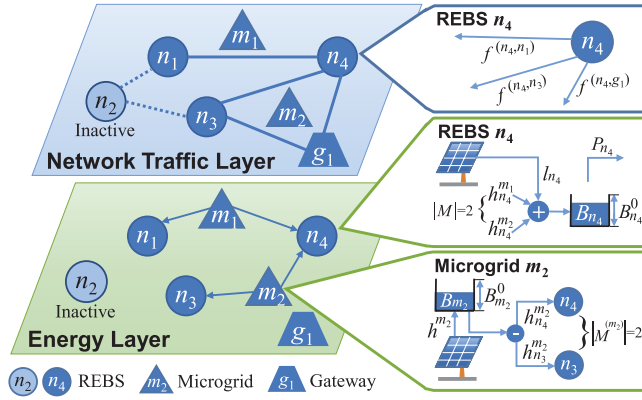


**FIGURE 2.** Traffic flow between REBSs, and energy flow inside REBSs and Microgrids.

Eq. 15-17 guarantee the non-gateway REBSs will send all allowed uplink and relayed data to the neighbors. The sign of  $f$  in Eq. 16 denotes traffic direction.

Fig. 2 particularizes the above-mentioned models. In the layer of network traffic, there are 5 REBSs and 2 Microgrids, the connected REBSs can mutually transfer the traffic. For example,  $n_4$  distributes traffic to  $n_1$ ,  $n_3$  and  $g_1$ , and can receive traffic from  $n_1$  and  $n_3$ . The energy layer denotes the relationship between Microgrids and REBSs.  $m_2$  distributes its energy to  $n_4$  and  $n_3$ , and the rest is stored locally. The available energy of  $n_4$  is the sum of energy from  $m_1$ ,  $m_2$ , its harvesting facility and the one stored in battery. After determining energy consumption, the rest will be stored in battery. Note that  $n_2$  does not operate and it disconnects the neighbors.

### G. THE METRIC FOR OPTIMIZATION

From Eq. 15-17, the local and remote data traffic for each REBS can finally arrive the network gateways. Therefore the system throughput in time slot  $t_i$ , we call it system utility  $U(t_i)$ , should be equal to the sum of local generated data traffic  $f_{n_j}(t_i)$ , as the following equation:

$$U(t_i) = \sum_{n_j \in \mathcal{N}} f_{n_j}(t_i). \quad (18)$$

There are several variables that determine equation (18), which are the operating status  $\rho_{n_j}(t_i)$ , energy allocation of each Microgrids  $h_{n_j}^{m_k}(t_i)$ , flow distribution  $f_{n_j}^{(n_j, n_k)}(t_i)$ , and the number of active subcarriers  $s_{n_j}(t_i)$ . Let  $\vec{\rho}$ ,  $\vec{h}$ ,  $\vec{f}$  and  $\vec{s}$  denote such variables respectively.

The total system utility in the considered time period  $\mathcal{T}$  is the sum of the system utility in each  $t_i$ . In light of the above analysis, the total system utility should be maximized by carefully choosing  $\vec{\rho}$ ,  $\vec{h}$ ,  $\vec{f}$  and  $\vec{s}$ :

$$U(\vec{\rho}, \vec{h}, \vec{f}, \vec{s}) = \sum_{t_i \in \mathcal{T}} U(t_i) = \sum_{t_i \in \mathcal{T}} \sum_{n_j \in \mathcal{N}} f_{n_j}(t_i). \quad (19)$$

The energy consumption should be taken into consideration since the energy is limited in disaster case. Moreover, the

diversities of the energy harvesting abilities of REBSs and Microgrids should also be reflected in the metrics. In this paper, we use the weighted energy consumption to represent the combination of energy consumption and the diversities. For REBS  $n_j$ , the weighted energy consumption  $\mathcal{W}_{n_j}^B$  is counted as follows:

$$\mathcal{W}_{n_j}^B = \frac{\sum_{t_i \in \mathcal{T}} (P_{n_j}(t_i) - \sum_{m_k \in \mathcal{M}} h_{n_j}^{m_k}(t_i))}{\sum_{t_i \in \mathcal{T}} l_{n_j}(t_i)}. \quad (20)$$

The denominator of Eq. 20 is the sum of the harvested energy of  $n_j$  during  $\mathcal{T}$ , and the numerator denotes the amount of energy from the battery and energy harvesting facility of  $n_j$ . For Microgrid  $m_k$ , the weighted energy consumption  $\mathcal{W}_{m_k}^M$  is calculated as follows:

$$\mathcal{W}_{m_k}^M = \frac{\sum_{t_i \in \mathcal{T}} \sum_{n_j \in \mathcal{M}^{(m_k)}} h_{n_j}^{m_k}(t_i)}{\sum_{t_i \in \mathcal{T}} h^{m_k}(t_i)}. \quad (21)$$

Its denominator represents the total amount of harvested energy of  $m_k$  in  $\mathcal{T}$ , the numerator is the total transmitted energy, which is utilized by its associated REBSs.

The optimization objective is to maximize the system utility in  $\mathcal{T}$ , and keep the sum of the weighted energy consumption as low as possible. Let  $\mathcal{D}$  be the set that contains all the solutions with the maximal total system utility, then the objective can be denoted as follows:

$$P1 : \min \sum_{n_j \in \mathcal{N}} \mathcal{W}_{n_j}^B + \sum_{m_k \in \mathcal{M}} \mathcal{W}_{m_k}^M, \quad (22)$$

where the definition domain is  $\mathcal{D}$ , and

$$\mathcal{D} = \{\mathbf{a} \mid \mathcal{U}(\mathbf{a}) \geq \mathcal{U}(\mathbf{b}), \text{ where } \mathbf{a} \neq \mathbf{b}, \text{ and } \mathbf{a}, \forall \mathbf{b} \in \text{dom}(\vec{\rho}, \vec{h}, \vec{f}, \vec{s})\}. \quad (23)$$

It is noted that a smaller slot length leads to a better system performance. This is because a finer granularity means a more timely adjustment toward the strategy. However, the sampling frequencies of traffic demand and energy input will rise up accordingly, which are neither effective, nor practical because one cannot get the information with an arbitrarily small degree and the performance boost introduced by a shorter slot length is limited. Moreover, it will increase the computational complexity since the number of variables becomes larger. In reality, considering the above issues, we set the sampling length be 1 hour as in [6] and [9].

### III. OFF-LINE SCHEME AND ON-LINE SCHEME

In this part, we firstly put forward a two-stage off-line scheme, which calculates problem P1 using expected estimation traffic. After that, based on the off-line result  $(\vec{\rho}, \vec{h}, \vec{f}, \vec{s})$ , we propose an on-line scheme that can dynamically adjust the result according to the available precise data traffic demands in each time slot.

#### A. TWO-STAGE OFF-LINE ENERGY EFFICIENT SCHEME

Problem P1 is a non-linear optimization problem since it contains non-linear constraints (i.e., Eq. 6). However, due to

the special structure of the problem, the non-linear constraints can be transferred into the linear ones. We introduce an extra variable,  $\delta_{n_j}(t_i)$ , which equals

$$\delta_{n_j}(t_i) = s_{n_j}(t_i) \cdot \rho_{n_j}(t_i). \quad (24)$$

And Eq. 6 becomes the following equation:

$$P_{n_j}(t_i) = e_0 \cdot \rho_{n_j}(t_i) + e_s \cdot \delta_{n_j}(t_i). \quad (25)$$

The detailed steps are similar to those in [19]. Using  $\delta_{n_j}(t_i)$ , problem P1 is then transformed into the problem with linear and integer constraints.

### 1) THE TWO-STAGE OFF-LINE ENERGY EFFICIENT SCHEME

In general, problem P1 finds the strategy with the lowest weighted energy consumption, from the set of solutions with the maximal total system utility. We use a two-stage scheme to solve P1 with expected data traffic demands. It is noted that the optimal result counted by proposed scheme is based on expected data traffic.

The first stage is to work out the maximal total system utility in  $\mathcal{T}$ . The objective and constraints are as follows:

$$\text{P2: } \tau = \max \sum_{t_i \in \mathcal{T}} U(t_i), \quad (26)$$

subject to constraints (1)-(5), (7)-(10), (13)-(17) and the transformed results of (6) and (12) by (24). P2 (Eq. 26) and constraints formulates an MILP problem and can be efficiently attacked by many existing solutions (i.e., branch and bound), since it only contains linear and integer constraints. Let  $\tau$  record the maximal total system utility of P2.

At the second stage, we use  $\tau$  as a constraint for P3, the objective and related constraints are as follows:

$$\text{P3: } \min \sum_{n_j \in \mathcal{N}} \mathcal{W}_{n_j}^B + \sum_{m_k \in \mathcal{M}} \mathcal{W}_{m_k}^M, \quad (27)$$

subject to

$$\sum_{t_i \in \mathcal{T}} U(t_i) = \tau, \quad (28)$$

as well as the related constraints. It is seen that P3 is also an MILP problem. By counting P2 and P3, we can eventually figure out the result for P1 in (22). This is because constraint (28) of P3 guarantees the result will have the maximal system utility (equals to  $\tau$ ), and the objective in (27) is to work out the minimum weighted power consumption, which is same as the requirement of (22) in essence. We denote this scheme as off-line scheme since it uses expectation traffic demands. The steps of this scheme are similar to the one in [19].

### 2) ANALYSIS ON THE OFF-LINE SCHEME

According to Eq. 11, there is an estimation deviation  $\epsilon_{n_j}(t_i)$  between the real data traffic demand and the expected one of REBS  $n_j$  in  $t_i$ . Such gap can be any value,

therefore  $\epsilon_{n_j}(t_i) \in (-\infty, +\infty)$ . We denote the positive part of the gap by  $[\epsilon_{n_j}(t_i)]^+$ :

$$[\epsilon_{n_j}(t_i)]^+ = \sup \{ \epsilon_{n_j}(t_i), 0 \}. \quad (29)$$

Let  $(\vec{\rho}^*, \vec{h}^*, \vec{f}^*, \vec{s}^*)$  denote the energy usage and traffic distribution strategy of P2 when we have the perfect data traffic demand information (we know real demand), and  $(\vec{\rho}', \vec{h}', \vec{f}', \vec{s}')$  be the related strategy using the expected data traffic demands. We have the following theorem:

*Theorem 1:* Let  $\tau^*$  be the maximal total system utility of the off-line result with  $(\vec{\rho}^*, \vec{h}^*, \vec{f}^*, \vec{s}^*)$ ,  $\tau'$  be the maximal total system utility of the off-line result calculated by  $(\vec{\rho}', \vec{h}', \vec{f}', \vec{s}')$ . When implementing the two strategies to deal with the real data traffic,  $\tau^*$  and  $\tau'$  will satisfy the following constraint:

$$0 \leq \tau^* - \tau' \leq \inf \left\{ \sum_{n_j \in \mathcal{N}} \sum_{t_i \in \mathcal{T}} [\epsilon_{n_j}(t_i)]^+, \tau^* \right\}. \quad (30)$$

*Proof:* Because  $(\vec{\rho}^*, \vec{h}^*, \vec{f}^*, \vec{s}^*)$  is the result of P2 when having perfect data traffic information. Since the proposed off-line result has the maximal total system utility, then  $\tau^*$  is not smaller than  $\tau'$ . Therefore the first inequality holds.

For the second inequality, define a vector  $\vec{d}$ , the elements of which are equal to:

$$\vec{d}_{n_j}(t_i) = \inf \{ d_{n_j}(t_i), \vec{d}_{n_j}(t_i) \}. \quad (31)$$

Let  $\tilde{\tau}$  be the maximal total system utility when the input data traffic demands are  $\vec{d}$ . Therefore,

$$\tau^* - \sum_{n_j \in \mathcal{N}} \sum_{t_i \in \mathcal{T}} [\epsilon_{n_j}(t_i)]^+ \leq \tilde{\tau} \leq \tau'. \quad (32)$$

According to the optimality of P2,  $\tilde{\tau}$  is the optimal result when the input data traffic demands are  $\vec{d}$ . Because the total data traffic demands gap between  $\vec{d}$  and  $d$  is:

$$d - \vec{d} = \sum_{n_j \in \mathcal{N}} \sum_{t_i \in \mathcal{T}} [\epsilon_{n_j}(t_i)]^+. \quad (33)$$

Therefore the first inequality of (32) holds. Because the solution space of P2 when input traffic is  $\vec{d}$ , is contained by the solution space of P2 when input traffic is  $d$ , therefore,  $\tilde{\tau} \leq \tau'$  and the second inequality of (32) holds.

Because of the correctness of (32), as well as the non-negative  $\tau'$ , the second inequality of (30) holds. ■

### B. PROPOSED ON-LINE DYNAMIC ADJUSTING SCHEME

The above off-line scheme will find the optimal solution if one can precisely predict the real data traffic. However, such strategy may not work well if the estimation deviation is notable (i.e.,  $[\epsilon_{n_j}(t_i)]^+$  is large). To deal with this problem, we put forward an on-line dynamic adjusting scheme.

In order to make use of the on-line scheme, we need to figure out the result of the off-line scheme once, before the execution of the on-line scheme for the first time (i.e., at the beginning of  $t_1$ ). Then the on-line scheme will be executed at

the beginning of each time slot. The adjusting plan given by the on-line scheme are recorded in three kinds of variables, their initial values are given as follows:

$$\begin{aligned} B_{n_j}^{Plan}(t_i) &= B_{n_j}(t_i), \forall t_i \in \mathcal{T}, n_j \in \mathcal{N}, \\ B_{m_k}^{Plan}(t_i) &= B_{m_k}(t_i), \forall t_i \in \mathcal{T}, m_k \in \mathcal{M}, \\ P_{n_j}^{Plan}(t_i) &= P_{n_j}(t_i), \forall t_i \in \mathcal{T}, n_j \in \mathcal{N}, \end{aligned}$$

where  $B_{n_j}^{Plan}(t_i)$ ,  $B_{m_k}^{Plan}(t_i)$  and  $P_{n_j}^{Plan}(t_i)$  are the residual energy of  $n_j$  in  $t_i$ , the residual energy of  $m_k$  in  $t_i$ , and the energy consumption of  $n_j$  in  $t_i$ , respectively. Such plan is initialized by the off-line scheme, and might be adjusted by the on-line scheme in each time slot. Let  $B_N^{Plan}$ ,  $B_M^{Plan}$ , and  $P_N^{Plan}$  be the set of  $B_{n_j}^{Plan}(t_i)$ ,  $B_{m_k}^{Plan}(t_i)$  and  $P_{n_j}^{Plan}(t_i)$ , respectively.

**Definition 1 (Maximal Available Spare Energy):** The maximal available spare energy  $\mathcal{E}_{n_j}(t_i)$  is the minimum value of  $B_{n_j}^{Plan}$ , from  $t_i$  to  $t_T$ :

$$\mathcal{E}_{n_j}(t_i) = \min_{t_i \leq t \leq t_T} B_{n_j}^{Plan}(t). \quad (34)$$

**Theorem 2:**  $\mathcal{E}_{n_j}(t_i)$  is the maximal available spare energy for  $n_j$  in  $t_i$  without affecting  $P_N^{Plan}$  from  $t_{i+1}$  to  $t_T$ .

*Proof:* According to Eq.7,  $B_{n_j}^{Plan}(t_{i+1}) \leq B_{n_j}^{Plan}(t_i)$  if  $P_{n_j}^{Plan}(t_i) \geq H_{n_j}(t_i)$ , otherwise  $B_{n_j}^{Plan}(t_{i+1}) > B_{n_j}^{Plan}(t_i)$ . Not to impact the strategy from  $t_{i+1}$  to  $t_T$ , the following inequalities should be satisfied:

$$\mathcal{E}_{n_j}(t_i) + P_{n_j}^{Plan}(t_{i+\alpha}) \leq H_{n_j}(t_{i+\alpha}) + B_{n_j}^{Plan}(t_{i+\alpha}), \quad (35)$$

for all  $\alpha \in \mathbb{Z}^+$  and  $0 \leq \alpha \leq T - i$ . In order to get the maximal available energy, at least one “=” of (35) should be satisfied. Therefore theorem 2 holds. ■

Note that Definition 1 and Theorem 2 are only for the REBSs, and it is simple to apply them to the case of Microgrids. We omit such parts due to lack of space.

Denote  $d(t_i) = \{d_{n_1}(t_i), d_{n_2}(t_i), \dots, d_{n_N}(t_i)\}$  as the real traffic demands of the REBSs in  $t_i$ . We use  $l$  and  $h$  to denote the total energy harvesting abilities of each REBS and Microgrid, respectively. After initializing  $B_N^{Plan}$ ,  $B_M^{Plan}$  and  $P_N^{Plan}$ , Algorithm 1 will be executed at the beginning of each time slot. In the following descriptions, we omit the time sequence number. In  $t_i$ , the on-line scheme firstly gets the real data traffic demands  $d$ , energy related information  $B_N^{Plan}$ ,  $B_M^{Plan}$ ,  $P_N^{Plan}$ ,  $l$ ,  $h$ , and topology information. The algorithm firstly calculates the maximal available spare energy  $\mathcal{E}_{n_j}$  of each  $n_j$  based on  $B_N^{Plan}$  and the energy received from Microgrids based on  $B_M^{Plan}$ , as shown by line 1 to 3. After getting the energy budget, the algorithm figures out  $\rho_{n_j}^{on\_temp}$  and  $s_{n_j}^{on\_temp}$  as the temporary operating status, and the maximal supporting subcarriers, respectively. We denote the set of REBSs in which the maximal available spare energy plus  $P_N^{Plan}$  can support the operation (i.e.,  $\mathcal{E} + P_N^{Plan} \geq e_0$ ), by  $\mathcal{N}_{avai}$ . Note that directly using  $\rho_{n_j}^{on\_temp}$  and  $s_{n_j}^{on\_temp}$  as the strategy may cause poor energy efficiency (i.e., some isolated REBSs may be in  $\mathcal{N}_{avai}$ ). Base on  $\rho_{n_j}^{on\_temp}$  and  $s_{n_j}^{on\_temp}$ , we calculate the

### Algorithm 1 On-line dynamic adjusting scheme

**Input:** Network topology information:  $G(\mathcal{N}, \mathcal{C})$ ,  $\mathcal{M}$ .

Energy information:  $B_N^{Plan}$ ,  $B_M^{Plan}$ ,  $P_N^{Plan}$ ,  $l$ ,  $h$ .

Traffic information:  $d$ .

**Output:**  $B_N^{Plan}$ ,  $B_M^{Plan}$ ,  $P_N^{Plan}$ ,  $(\rho^{on}, h^{on}, f^{on}, s^{on})$ .

- 1 Figure out the maximal available spare energy  $\mathcal{E}_{n_j}$  for each  $n_j$  according to equation 37;
- 2 For each  $m_k$ , **if**  $n_j \in M^{(m_k)}$  **then**
- 3      $\mathcal{E}_{n_j} = \mathcal{E}_{n_j} + \min_{t_T \geq t \geq t_i} \{B_{m_k}^{Plan}(t)\} / |M^{(m_k)}|$ ;
- 4 For each  $n_j$ , set  $\rho_{n_j}^{on\_temp}$  and  $s_{n_j}^{on\_temp}$  by (6):  

$$\arg \max_{s_{n_j}^{on\_temp} \leq S, \rho_{n_j}^{on\_temp} \in (0,1)} \{P'_{n_j} | P'_{n_j} \leq \mathcal{E}_{n_j} + P_N^{Plan}\};$$
- 5 Let  $\mathcal{N}_{avai} = \{n | n \in \mathcal{N} \text{ and } \rho_n^{on\_temp} == 1\}$ ;
- 6 Base on  $d$ ,  $\rho_{n_j}^{on\_temp}$  and  $s_{n_j}^{on\_temp}$ , figure out the maximal system utility  $U^{on}$  in current time slot;
- 7 Initialize  $cur\_Node = \{\mathcal{G}\}$ ,  $ava\_Node = \mathcal{N}_{avai} - \{\mathcal{G}\}$ ;
- 8 Set  $Utility = 0$ ;
- 9 **while**  $True$  **do**
- 10     **if**  $Utility == U^{on}$  **then**
- 11         Set  $\rho^{on}$  according to  $cur\_Node$ ;
- 12         Use  $\rho^{on}$ ,  $l$ ,  $h$  and  $\tau = U^{on}$ , and assume in P3  $s$  can be real value, to figure out P3. We will obtain  $s_{real}^{on}, f^{on}, h^{on}$ ;
- 13         Let  $s^{on}$  be  $\lceil s_{real}^{on} \rceil$ ;
- 14         Use  $P_N^{Plan}$  to record the energy consumption plan, and update  $B_N^{Plan}$  and  $B_M^{Plan}$  for the left time slots according to  $P_N^{Plan}$ ;
- 15         **return**  $B_N^{Plan}$ ,  $B_M^{Plan}$ ,  $P_N^{Plan}$ , and  $(\rho^{on}, h^{on}, f^{on}, s^{on})$ ;
- 16     Choose  $n_{max} \in ava\_Node$  that the system utility is maximized, with the assumptions that only REBSs in  $\{n_{max}\} \cup cur\_Node$  are active, and the number of active subcarriers are given by  $s_{n_j}^{on\_temp}$ . Let  $U_{max}$  be the maximal system utility;
- 17      $Utility = U_{max}$ ,  $cur\_Node = cur\_Node \cup \{n_{max}\}$ ,  
 $ava\_Node = ava\_Node \setminus \{n_{max}\}$ ;

maximal system utility  $U^{on}$ . After that, the algorithm tries to find the most energy-efficient strategy: we iteratively choose the REBS from the available REBSs ( $ava\_Node$ ), in order to enlarge the set of considered REBSs ( $cur\_Node$ ) in a greedy manner. In each iterative step, we firstly choose the REBS from  $ava\_Node$  with the most system utility improvements, and add it to  $cur\_Node$ . Such iteration will stop when current system utility equals  $U^{on}$ . After that, the system will figure out the most energy-efficient results  $(\rho^{on}, h^{on}, f^{on}, s^{on})$ , with the constraint of the system utility  $U^{on}$  according to  $cur\_Node$  using Eq.22. At last,  $B_N^{Plan}$ ,  $B_M^{Plan}$ , and  $P_N^{Plan}$  will be updated, and  $(\rho^{on}, h^{on}, f^{on}, s^{on})$  will be given by the on-line result. Line 9 to 17 describe this procedure. From Theorem 2, it can be seen that in each time slot, the available energy for each REBS of the on-line scheme will be equal or greater than

the one of the off-line scheme, therefore the system utility of the on-line scheme will be at least same as the one of the off-line scheme.

#### IV. PERFORMANCE EVALUATION

In this section, we examine the performance of the proposal through computer-based simulations. We mainly compare the following schemes: proposed off-line two stage energy efficient scheme with perfect data traffic demand information (Off-line with perfect information), the off-line scheme only with expected data traffic demands (Off-line with expected information), and the off-line scheme combined with on-line scheme using expected data traffic information (Off-line combined with on-line). The parameters are listed in Table 1.

**TABLE 1. Experimental parameters.**

Parameter	Value
$t_0$	1 hour
The number of considered time slots ( $T$ )	5
Number of REBSs ( $N$ )	11
Number of Microgrids ( $M$ )	3
Number of gateways ( $F$ )	2
Bandwidth of the Backhaul link ( $c_{n_j}^{n_k}$ )	80 to 300Mbps
Operating power consumption ( $e_0$ )	712.2W
Power consumption per each subcarrier ( $e_s$ )	1.06W
Number of subcarriers $S$	600
Battery capacity of $B_{n_j}^0$ and $B_{m_k}^0$	2000W
Rate of subcarriers $r_0$	0.5Mbps

In order to testify the importance of the long-term optimization, we also examine the performances of Naive scheme (Naive). The Naive idea does not consider saving the energy for future use. In general, Naive idea focuses on system utility as well as keeping weighted energy consumption at a low level. For the Microgrids, in each time slot, they evenly send their maximal available energy to connected REBSs. For each REBS, it firstly calculates its operating status and active subcarriers according to the available energy in each time slot. After that, it employs the procedure like line 6 to 16 in algorithm 1, to figure out the most system utility with the lowest energy consumption. It can be seen that the steps of Naive idea is similar to on-line scheme, and the major difference between Naive idea and on-line scheme is the latter one has guidance of off-line scheme.

As table 1 shows, time slot length is 1 hour. We consider the scenario with 11 REBSs ( $N = 11$ ), in which there are 2 gateways ( $F = 2$ ). Each REBS connects to its neighbors by microwave panel or long distance WiFi. The bandwidth of the link connecting two neighboring REBSs is randomly chosen from 80Mbps to 300Mbps, according to the parameters of commercial products. In simulations, we assume these REBSs are macro base stations. Based on the measurement in [9], we set  $e_0 = 712.2W$ ,  $e_s = 1.06W$  and  $S = 600$ . The battery capacity is set as 2kW, and we assume the initial energy in battery of each REBS equals the battery capacity. Every 60 subcarriers is regarded as an active unit, which means these subcarriers are simultaneously active or inactive.

In the remainder of this section, we mainly investigate our proposed schemes by two performance metrics, namely

total system throughput and weighted energy consumption per megabit. The former is same as the total system utility mentioned in previous sections, and the latter is the quotient of weighted energy consumption in Eq. 22, divided by its associated system throughput in Eq. 19. Topology of the network in the simulations is shown in Fig. 3.

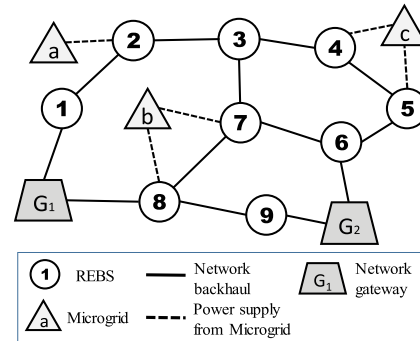


**FIGURE 3. System topology used in performance evaluation.**

#### A. EFFECT OF THE ESTIMATION ERROR OF DATA TRAFFIC DEMANDS ON SYSTEM THROUGHPUT

Firstly, we study the impact of the estimation error of data traffic demands. For each REBS, we suppose the average energy input is randomly chosen from interval [100W, 300W], and the average expected data traffic demands is randomly chosen from interval [20Mbps, 50Mbps].

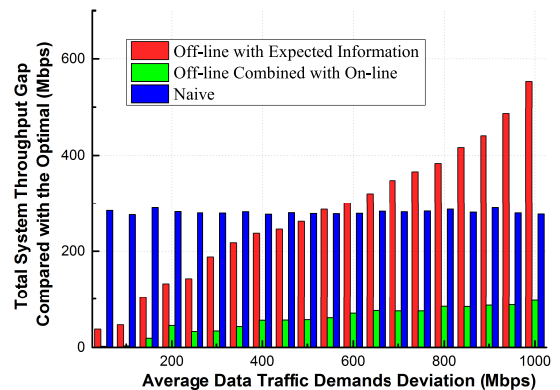


**FIGURE 4. The effect of  $\epsilon$  on system throughput of the off-line with expected information, off-line combined with on-line, and Naive scheme.**

Fig. 4 demonstrates the change of the total system utility gap between the three schemes and the optimal result (off-line with perfect information), with the estimation error. The X axis denotes the estimation deviation  $\epsilon$ , and  $\sum[\epsilon]^+ = \sum[\epsilon]^- = x$ . It can be seen that as the estimation deviation increases, the performance of the scheme that only uses the expected traffic will decrease (the gap becomes larger), because the off-line scheme tends to give a worse strategy when such deviation becomes larger. The scheme that combines the off-line and on-line, on the other hand, has a less system utility loss when the estimation error



is large. The Naive idea is used as a comparison, and its performance is independent with traffic prediction, because it always gets the current-optimal result in a greedy manner. When the total estimation deviation is larger than 600Mbps, the system utility of the off-line result using expected data traffic information will be worse than the Naive idea.

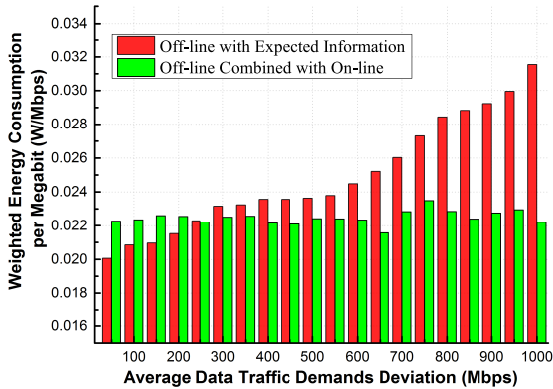


FIGURE 5. The effect of  $\epsilon$  on energy efficiency of the off-line with expected information and off-line combined with on-line scheme.

Fig. 5 depicts the comparison of the energy efficiency of the two schemes. From Fig. 5, the consumed energy per megabit is proportional to the estimation deviation for off-line scheme with expected information. This is because if one only considers the expected data traffic demands, as estimation deviation increases, the system throughput will decrease while the energy consumption remain unchanged. As a comparison, if we combine off-line result with the on-line one, then energy can be used in a more flexible way: when experiencing low traffic, unnecessary subcarriers will be shut down; when the traffic is higher than expectation, we can use the extra energy to activate more subcarriers and/or more REBSs. When  $\epsilon$  is small, the energy efficiency of the off-line with expected information is better than the on-line combined with off-line. This is because the affect of estimation error on performance is not significant when  $\epsilon$  is small: since the off-line scheme can figure out the optimal result, and the extra throughput achieved by on-line scheme will cost much energy, the energy efficiency is therefore unsatisfied. When total  $\epsilon$  is larger than 250Mbps, using expected information cannot guarantee the system throughput and is therefore inefficient. From Fig. 4 and Fig. 5, the proposed optimal solution can efficiently deal with estimation deviation of the data traffic demands.

### B. EFFECT OF TOTAL AVAILABLE ENERGY ON SYSTEM THROUGHPUT AND ENERGY CONSUMPTION

In this part, we vary the input renewable energy and try to observe its impact on system utility and energy efficiency. For each REBS, the real renewable energy input in each time slot is uniformly and randomly chosen from interval  $[0.5 * \text{average input energy}, 1.5 * \text{average input energy}]$ . The

data traffic demand for each REBS in each time slot is uniformly and randomly chosen from interval  $[20\text{Mbps}, 60\text{Mbps}]$ . We set  $\sum[\epsilon]^+ = 200\text{Mbps}$  and  $\sum[\epsilon]^- = 200\text{Mbps}$ . Other experiment parameters are set as table 1.

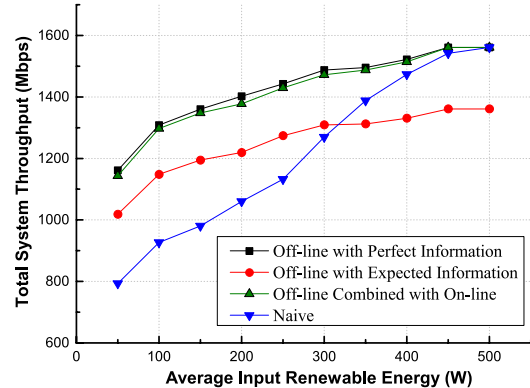
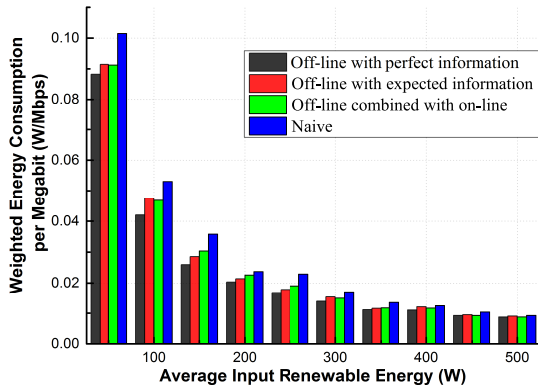


FIGURE 6. The effect of average input renewable energy on system throughput of the four schemes.

Fig. 6 illustrates the change of the system throughput, with the average input rate of the renewable energy of each REBS and Microgrids. As Fig. 6 shows, the total system throughput is in general proportional to the average harvested energy for each scheme, this is because as more energy is available, comparatively longer operating time and more active subcarriers can be supported for each REBS, then more traffic can be delivered to the destination. The estimation error causes a clear performance gap between the off-line with expected information and the optimal result. Note that the performance gap between the on-line scheme and the optimal one is small within the measuring range. Compared with the myopic Naive scheme, the on-line scheme has a better system utility: if the REBS consumes too much energy in current time, the lack of energy in future will potentially reduce its throughput. It is worthwhile to note that when the input renewable energy is more than 450W per each REBS, the throughput keeps at the peak point for the two schemes, this is because before 450W, the bottleneck of the network is the input energy, and after 450W, the input traffic and network capacity become the bottleneck. Such phenomenon reveals the importance of considering both of the two bottlenecks in disaster case.

Fig. 6 also provides an interesting result: when average input renewable energy is less than 300W, the off-line with expected information scheme has a larger system utility, after this value, it is outperformed by Naive scheme. As input energy increases, the energy becomes sufficient and the optimal strategy will gradually become the same as the Naive one, which is to pursue the current maximal system utility in each time slot. For the off-line with expectation information, the system utility will not rise even the input energy is high enough, because of the negligence on data estimation error.

Fig. 7 demonstrates the energy efficiencies of the four schemes. As the input renewable energy increases, the



**FIGURE 7.** The effect of average input renewable energy on consumed power per megabit of the four schemes.

weighted energy consumption of the four schemes decreases. The main reason is, the constant operating energy consumption will not directly improve system throughput. It is the active subcarriers that collect the data traffic demands contribute to utility. Therefore the larger energy consumption ratio of the active subcarriers, the more efficient such energy can be utilized. It can be seen that the energy efficiency of the Naive idea is worse than the others'. This is because the Naive idea only pursue the current maximal system utility, which leads to an unsatisfied utilization of the input energy.

### C. EFFECT OF TOTAL TRAFFIC DEMANDS ON SYSTEM THROUGHPUT AND ENERGY CONSUMPTION

In this part, we put traffic demands as the variables. The traffic demands for the REBSs in each time slot are uniformly and randomly chosen from interval  $[0.5 * \text{average input traffic}, 1.5 * \text{average input traffic}]$ . The renewable energy input for each REBS in each time slot is also uniformly and randomly chosen from interval  $[100W, 300W]$ . We set  $\sum[\epsilon]^+ = 200\text{Mbps}$  and  $\sum[\epsilon]^- = 200\text{Mbps}$ . Other parameters are set as table 1.

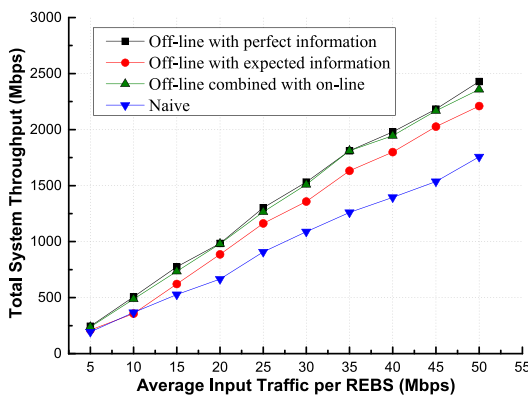


**FIGURE 8.** The effect of average input traffic per REBS on total system throughput of the four schemes.

Fig. 8 demonstrates the effects of average input traffic per REBS on total systems throughput of the four schemes.

From Fig. 8, traffic demand is proportional to the total system utility, and the proposed on-line scheme can achieve almost same total system utility as the optimal one. Because of estimation error, there is a clear performance gap between off-line with expected information scheme and the optimal one. The Naive idea has the worst performance among these four schemes. As the data traffic demands increase, the performance gap between the Naive idea and the other three schemes becomes larger. The reason is, when energy input is fixed, the method for utilizing limited energy determines the final result, and such influence will become more prominent as the input data traffic demands increase.

Fig. 9 shows the comparison of the consumed power per megabit of the four schemes. It is apparent that the energy efficiency is proportional to input data traffic. When input traffic is low, the major energy is used for the constant operation, which means the system uses a large amount of energy to transmit a small amount of data, and then causes the inefficiency. As input traffic increases, before network capacity reaching saturation, REBS can simply transfer more traffic only at the cost of subcarrier energy consumption, which is much smaller than the constant consumption. This result shows that the more energy used for subcarrier, the better energy efficiency that we can achieve.

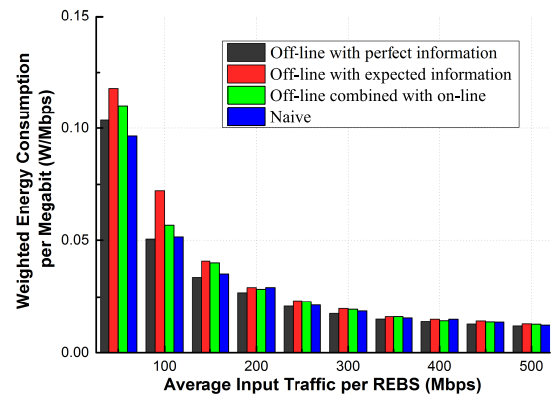


**FIGURE 9.** The effect of average input traffic per REBS on consumed power per megabit of the four schemes.

## V. CONCLUSION

This paper focuses on the energy-efficient throughput-optimization problem for the Wireless Mesh Networks (WMNs) composed of Renewable Energy-enabled Base Stations (REBSs) in disaster area. In order to provide the maximal system throughput and keep the energy consumption at a low level, we propose an off-line scheme that takes energy-harvesting profile into consideration to achieve the energy-efficient result. We firstly formulates a throughput-maximization problem, then figures out the maximal throughput. Then we figure out the most energy-efficient result while guaranteeing the maximal network throughput. We also propose an on-line scheme, which can dynamically adjust the result of the off-line scheme based on the real traffic

information. Theoretical and numerical results show that our proposed off-line energy efficient scheme can achieve high system throughput, as well as high energy efficiency when traffic prediction is relative precise, and the on-line scheme can guarantee the system performances even if prediction error is relative large.

**REFERENCES**

[1] A. Kwasinski, W. W. Weaver, P. L. Chapman, and P. T. Krein, "Telecommunications power plant damage assessment for hurricane Katrina—Site survey and follow-up results," *IEEE Syst. J.*, vol. 3, no. 3, pp. 277–287, Sep. 2009.

[2] A. Kwasinski, "Effects of notable natural disasters from 2005 to 2011 on telecommunications infrastructure: Lessons from on-site damage assessments," in *Proc. IEEE 33rd Int. Telecommun. Energy Conf. (INTELEC)*, Oct. 2011, pp. 1–9.

[3] T. Sakano et al., "Disaster-resilient networking: A new vision based on movable and deployable resource units," *IEEE Netw.*, vol. 27, no. 4, pp. 40–46, Jul. 2013.

[4] A. Kwasinski and A. Kwasinski, "Architecture for green mobile network powered from renewable energy in microgrid configuration," in *Proc. IEEE Wireless Commun. Netw. Conf. (WCNC)*, Apr. 2013, pp. 1273–1278.

[5] K. Heimerl, K. Ali, J. Blumenstock, B. Gawalt, and E. Brewer, "Expanding rural cellular networks with virtual coverage," in *Proc. 10th USENIX Symp. Netw. Syst. Design Implement. (NSDI)*, Lombard, IL, USA, 2013, pp. 283–296.

[6] A. Fernandez, Y. Gala, and J. R. Dorronsoro, "Machine learning prediction of large area photovoltaic energy production," in *Proc. 2nd Workshop Data Anal. Renew. Energy Integr. (DARE)*, Nancy, France, Sep. 2014, pp. 38–53.

[7] M. A. Marsan, L. Chiaraviglio, D. Ciullo, and M. Meo, "On the effectiveness of single and multiple base station sleep modes in cellular networks," *Comput. Netw.*, vol. 57, no. 17, pp. 3276–3290, 2013.

[8] O. Arnold, F. Richter, G. Fettweis, and O. Blume, "Power consumption modeling of different base station types in heterogeneous cellular networks," in *Proc. Future Netw. Mobile Summit*, Jun. 2010, pp. 1–8.

[9] G. Auer et al., "Cellular energy efficiency evaluation framework," in *Proc. IEEE 73rd Veh. Technol. Conf. (VTC Spring)*, May 2011, pp. 1–6.

[10] T. Han and N. Ansari, "Optimizing cell size for energy saving in cellular networks with hybrid energy supplies," in *Proc. IEEE Global Commun. Conf. (GLOBECOM)*, Dec. 2012, pp. 5189–5193.

[11] M. Gatzianas, L. Georgiadis, and L. Tassioulas, "Control of wireless networks with rechargeable batteries [transactions papers]," *IEEE Trans. Wireless Commun.*, vol. 9, no. 2, pp. 581–593, Feb. 2010.

[12] W. Guo and T. O'Farrell, "Green cellular network: Deployment solutions, sensitivity and tradeoffs," in *Proc. Wireless Adv. (WiAd)*, Jun. 2011, pp. 42–47.

[13] G. Miao, N. Himayat, G. Y. Li, and S. Talwar, "Low-complexity energy-efficient scheduling for uplink OFDMA," *IEEE Trans. Commun.*, vol. 60, no. 1, pp. 112–120, Jan. 2012.

[14] L. X. Cai, Y. Liu, T. H. Luan, X. Shen, J. W. Mark, and H. V. Poor, "Sustainability analysis and resource management for wireless mesh networks with renewable energy supplies," *IEEE J. Sel. Areas Commun.*, vol. 32, no. 2, pp. 345–355, Feb. 2014.

[15] M. X. Cheng, X. Gong, L. Cai, and X. Jia, "Cross-layer throughput optimization with power control in sensor networks," *IEEE Trans. Veh. Technol.*, vol. 60, no. 7, pp. 3300–3308, Sep. 2011.

[16] M. F. Mostafa, H. Nishiyama, R. Miura, and N. Kato, "On efficient traffic distribution for disaster area communication using wireless mesh networks," *Wireless Personal Commun.*, vol. 74, no. 4, pp. 1311–1327, Feb. 2014.

[17] S. Guo, L. T. Yang, G. Min, and X. Xie, "Green communication in energy renewable wireless mesh networks: Routing, rate control, and power allocation," *IEEE Trans. Parallel Distrib. Syst.*, vol. 99, p. 1, 2014.

[18] T. Ngo, H. Nishiyama, N. Kato, T. Sakano, and A. Takahara, "A spectrum- and energy-efficient scheme for improving the utilization of MDRU-based disaster resilient networks," *IEEE Trans. Veh. Technol.*, vol. 63, no. 5, pp. 2027–2037, Jun. 2014.

[19] M. Li, H. Nishiyama, Y. Owada, and K. Hamaguchi, "On energy efficient scheduling and load distribution based on renewable energy for wireless mesh network in disaster area," in *Proc. 13th IEEE Int. Conf. Trust, Security Privacy Comput. Commun. (TrustCom)*, Sep. b2014, pp. 465–472.

[20] J. Lu, S. Liu, Q. Wu, and Q. Qiu, "Accurate modeling and prediction of energy availability in energy harvesting real-time embedded systems," in *Proc. Int. Green Comput. Conf.*, Aug. 2010, pp. 469–476.

[21] S. He, J. Chen, F. Jiang, D. K. Y. Yau, G. Xing, and Y. Sun, "Energy provisioning in wireless rechargeable sensor networks," in *Proc. IEEE INFOCOM*, Apr. 2011, pp. 2006–2014.

[22] J. Chen, X. Cao, P. Cheng, Y. Xiao, and Y. Sun, "Distributed collaborative control for industrial automation with wireless sensor and actuator networks," *IEEE Trans. Ind. Electron.*, vol. 57, no. 12, pp. 4219–4230, Dec. 2010.

[23] H. Li, L. Song, and M. Debbah, "Energy efficiency of large-scale multiple antenna systems with transmit antenna selection," *IEEE Trans. Commun.*, vol. 62, no. 2, pp. 638–647, Feb. 2014.

[24] X. Wang and L. Cai, "Stability region of opportunistic scheduling in wireless networks," *IEEE Trans. Veh. Technol.*, vol. 63, no. 8, pp. 4017–4027, Oct. 2014.



**MENG LI** (S'13) received the B.E. degree from Lanzhou University, Lanzhou, China, in 2009, and the M.E. degree from the University of Science and Technology of China, Hefei, China, in 2012. He is currently pursuing the Ph.D. degree with the Graduate School of Information Sciences, Tohoku University, Sendai, Japan. His main research interests include resource allocation and cellular networks. He has received the Best Paper Awards from the IEEE TrustCom in 2014.



**HIROKI NISHIYAMA** (SM'13) received the M.S. and Ph.D. degrees in information science from Tohoku University, Sendai, Japan, in 2007 and 2008, respectively, where he is currently an Associate Professor with the Graduate School of Information Sciences. He has authored over 120 peer-reviewed papers, including many high-quality publications in prestigious IEEE journals and conferences. One of his outstanding achievements is Relay-by-Smartphone, which makes it

possible to share information among many people using only Wi-Fi functionality of smartphones. His research interests include satellite communications, unmanned aircraft system networks, wireless and mobile networks, ad hoc and sensor networks, green networking, and network security. He is a member of the Institute of Electronics, Information, and Communication Engineers (IEICE) and the Secretary of the IEEE Communication Society Sendai Chapter. He serves as an Associate Editor of the IEEE TRANSACTIONS ON VEHICULAR TECHNOLOGY and the *Peer-to-Peer Networking and Applications* (Springer) journal. He will serve as the Co-Chair of the Cognitive Radio and Networks Symposium of the IEEE International Conference on Communications (ICC) in 2015. He has served as the Co-Chair of the Selected Areas in Communications Symposium of the IEEE ICC in 2014. He has received several Best Paper Awards from many international conferences, including the IEEE's flagship events, such as the IEEE Global Communications Conference in 2010 and 2013 and the IEEE Wireless Communications and Networking Conference in 2012 and 2014. He was a recipient of the FUNAI Foundation's Research Incentive Award for Information Technology in 2009, the IEICE Communications Society Academic Encouragement Award in 2011, and the IEEE Communications Society Asia-Pacific Board Outstanding Young Researcher Award in 2013.



**NEI KATO** (M'03–SM'05–F'13) received the M.S. and Ph.D. degrees in information engineering from Tohoku University, Sendai, Japan, in 1988 and 1991, respectively. He has been involved in research on computer networking, wireless mobile communications, satellite communications, ad hoc and sensor and mesh networks, smart grid, and pattern recognition. He currently serves as a Member-at-Large on the Board of Governors of the IEEE Communications Society, the Chair of the IEEE Ad Hoc and Sensor Networks Technical Committee, the Chair of the IEEE ComSoc Sendai Chapter, an Associate Editor-in-Chief of the IEEE INTERNET OF THINGS JOURNAL, an Area Editor of the IEEE TRANSACTIONS ON VEHICULAR TECHNOLOGY, and an Editor of the IEEE WIRELESS COMMUNICATIONS MAGAZINE and the IEEE NETWORK MAGAZINE. He has served as the Chair of the IEEE ComSoc Satellite and Space Communications Technical Committee (2010–2012), the Chair of the IEICE Satellite Communications Technical Committee (2011–2012), a Guest Editor of many IEEE TRANSACTIONS/journals/magazines, the Symposium Co-Chair of GLOBECOM (2007), the IEEE International Conference on Communications (ICC) (2010), ICC (2011), and ICC (2012), the Vice Chair of the IEEE WCNC (2010), WCNC (2011), ChinaCom (2008), and ChinaCom (2009), the Symposia Co-Chair of GLOBECOM (2012), the TPC Vice Chair of ICC (2014), and the Workshop Co-Chair of VTC (2010). He was a recipient of the IEICE Network System Research Award (2009), the IEICE Satellite Communications Research Award (2011), the KDDI Foundation Excellent Research Award (2012), the IEICE Communications Society Distinguished Service Award (2012), the Distinguished Contributions to Disaster-Resilient Networks Research and Development Award from the Ministry of Internal Affairs and Communications, Japan, six Best Paper Awards from the IEEE GLOBECOM/WCNC/VTC, and the IEICE Communications Society Best Paper Award (2012). Besides his academic activities, he also serves on the Expert Committee of the Telecommunications Council, the Ministry of Internal Affairs and Communications, and as the Chair of ITUR SG4 and SG7 in Japan. He is a Distinguished Lecturer of the IEEE Communications Society and the Vehicular Technology Society.



**YASUNORI OWADA** (M'03) received the bachelor's degree in biocybernetics, the master's degree in engineering, and the Ph.D. degree in electronics and electrical communications from Niigata University, Niigata, Japan, in 2002, 2004, and 2007, respectively. He is currently an Expert Researcher with the National Institute of Information and Communications Technology, Sendai, Japan. He is currently a member of the AKARI Architecture Design Project. He is involved in designing wireless access network architecture of future mobile and sensor networks. He is investigating the research challenges of wireless resources sensing, allocations and management architecture, cross-layer interactions, and routing in wireless multihop networks. He was involved in the standardization of a mobile ad hoc network routing protocol at IETF, Yokohama, Japan, from 2004 to 2008. He was involved in the development of a wireless network simulator with Space-Time Engineering Japan, Inc., Wako, Japan, as the President, from 2008 to 2010. He was a recipient of the IEICE Young Researcher's Award in 2003. He is a member of the Information Processing Society of Japan.



**KIYOSHI HAMAGUCHI** (M'00) received the B.E. and M.E. degrees in electrical engineering from the Tokyo University of Science, Tokyo, Japan, in 1989 and 1991, respectively, and the D.Eng. degree from Osaka University, Osaka, Japan, in 2000. Since 1993, he has been with the National Institute of Information and Communications Technology (NICT), Sendai, Japan, where he has been involved in research and development of wireless telecommunication technologies, including a land mobile data communication system, a millimeter-wave data transmission system, an ultrawideband device, and a medical ICT system and applications. From 2002 to 2003, he was a Visiting Researcher with the University of Southampton, Southampton, U.K. He is currently the Director of the Wireless Mesh Network Laboratory with the Resilient ICT Research Center, NICT. He was a recipient of the Young Engineer Award from the Institute of Electronics, Information, and Communication Engineers (IEICE) in Japan in 1997, the Young Scientist Award from the Ministry of Education, Culture, Sports, Science and Technology in Japan in 2006, and the Radio Achievement Award from ARIB in Japan in 2010. He is a member of IEICE.